Dissolution kinetics of α phase in TA6V titanium alloy

Moukrane Dehmas[1], Richard Katemi[1], Benoît Appolaire[2], Elisabeth Aeby-Gautier[1], Benoit Denand[1], Sylvain Audion[3]

[1]*Institut Jean Lamour, SI2M, Ecole des Mines, Parc de Saurupt, 54042 Nancy France*
[2]*ONERA, LEM, 29, avenue de la Division Leclerc, 92322 Chatillon France*
[3]*AIRBUS, 316, Route de Bayonne, BP E5001 31060 Toulouse Cedex 9*

Abstract: The complexity and diversity of microstructure involved in titanium alloys make it rather difficult to quantitatively describe microstructural evolution. In the present study we focus on microstructure evolutions during heating and isothermal holding considering the effect of the initial microstructure on the dissolution kinetics of α phase. Quantitative microstructure characterizations have been realized. At first, in situ high energy X-ray synchrotron and electrical resistivity was used to follow the dissolution kinetics of α phase. Then, an algorithm capable of quantifying various microstructural data was developed. The microstructural features include the amount of nodular and lamellar α phase, the mean equivalent diameter and the aspect ratio of nodular α phase. This algorithm was applied to TA6V4 samples submitted to different isothermal temperature. The initial microstructure of the samples was either a duplex microstructure (lamellar and nodular α phase) or a nodular microstructure. The dissolution kinetics of α phase was compared with the equilibrium calculations predicted by ThermoCalc. It appears clearly that a large amount of α phase is dissolved on heating in spite of a rapid heating rate.

Keywords: TA6V, dissolution kinetics, synchrotron diffraction, image analysis, modeling

1. Introduction

It is widely known that the mechanical properties in titanium alloys are essentially due to the various microstructures and microtextures that form during thermal and/or thermomechanical treatments (TMT). For example, titanium alloy with a duplex microstructure offers advantage in term of yield strength, tensile strength[1)], while the presence of nodular α precipitates increases the tensile elongation (plasticity).

In order to improve the TMT it is necessary to understand and model the microstructures evolutions. Numeric tools are thus developed to predict the microstructure formation and evolution[2)]. The validation of these tools needs accurate measurements of various features of the microstructure (kinetics[4)] as morphology changes[3)]). In the case of TA6V titanium alloy, it is commonly admitted that the dissolution and growth kinetics of α phase during isothermal holding and cooling is very quick[5)]. However, only few data[6)] report on the dissolution kinetics of α phase for high heating rate, as on the incidence of the initial morphology of α phase.

In the present we investigate the dissolution kinetics of α phase on heating with a high heating rate and during isothermal holding for two initial microstructures (i.e fully nodular and duplex (lamellar and nodular)). Kinetics is characterized by time-resolved in situ X-ray diffraction[4)] and electrical resistivity. In addition, morphologic features are measured at room temperature by quantitative image analyses on samples quenched after different isothermal holdings. The experimental results will be discussed in regard of the equilibrium calculations.

2. Materials and methods

The alloy provided by TIMET UK was a commercial Ti-6Al-4V (TA6V) titanium alloy. Its composition (in wt.%) is 6.4Al, 4.0V, 0.14Fe, 0.19O and balance Ti. The β transus temperature (T_β) was determined via the electrical resistivity measurements to be 995°C. Two as-received states were studied. The first was an as-extruded state, delivered in a cylinder form with a diameter of 20 mm. The second one was an as-forged state, delivered as a billet with a diameter of 200 mm. The specimens (diameter of 4 mm and a length of 40 mm) were machined from each as-received material. Heat treatments were conducted on these specimens by a device developed in the laboratory, which allows recording in real time the electrical resistivity. The specimens were heated with a heating rate of 10°C/s at different temperatures for 1 hour, and further cooled to room temperature by helium blowing. The holding temperatures were T_β-25°C, T_β-40°C, T_β-70°C et T_β-125°C for the F state and T_β-40°C for the E state.

After quenching, the microstructure of each sample was imaged by SEM with a Philips XL30 SFEG. Quantitative image analysis was conducted on at least 20 images/sample to determine different microstructural features i.e. the amount of nodular and lamellar α phase, the mean equivalent diameter and the aspect ratio of nodular α phase. On the grey scale of BSE images, the α phase can be distinguished from β phase due to the brighter contrast arising from its higher average atomic number that is illustrated on Figure 1a. Nodular grains were analyzed after thresholding, and several steps of erosion and reconstruction to eliminate the lamellar precipitates. The watershed algorithm was then used to separate adjoined nodular shapes (Figure 1b). After this step, the extracted features were the number density of nodular phase. For the determination of mean equivalent diameter and shape factor, the particles that are connected to the image borders are eliminated (Figure 1c). To quantify the amount of lamellar phase, a NAND logical operator was used to keep only the α lamellar (Figure 1d).

To get a quantitative measurement of phase amounts, XRD experiments were done at the European Synchrotron Radiation Facility (ESRF) in Grenoble (France) on the ID15B beam line. The in situ measurements were performed by high energy X-ray synchrotron diffraction (HEXRD) with a monochromatic

beam of 89 keV (beam size 400 x 400 µm^2). The experimental device consists of a radiant furnace with an argon atmosphere in which the sample is mounted on a rotating sample holder. During the heat treatments, the temperature was measured by a type S thermocouple spot welded on the sample surface and close to the analysed volume. A Pixium 2D image plate detector (2640 x 1920), placed at 1039 mm from the sample allows recording a complete collection of the Debye-Scherrer rings. These rings were acquired every 3.5 s. In order to obtain the classical 2θ scans suitable for Rietveld analysis, the intensity of each ring was integrated.

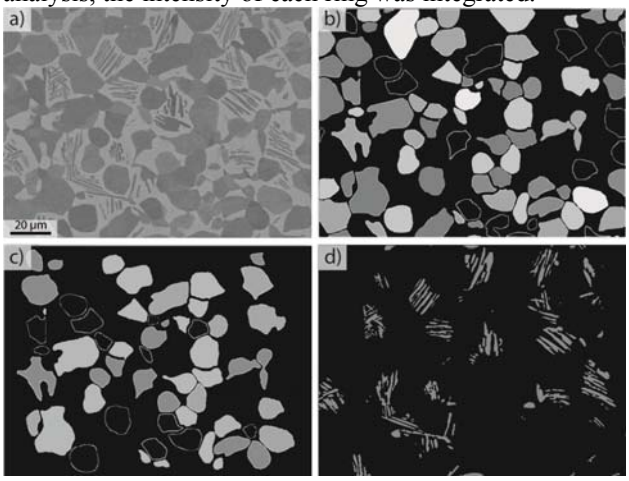

Figure 1. Illustration of the automatic identification of lamellar and nodular morphologies: a) original backscattered image; b) segmentation of nodular morphology after application of the watershed method; c) border kill; d) quantification of lamellar morphology.

3. Results

3.1 As-received microstructures

The microstructures at the as-received states are shown in Figure 2. The as-extruded state has a nodular α phase surrounded by a small amount of remaining β matrix (Figure 2a). A duplex microstructure is observed for the as-forged state (Figure 2b) with nodular α phase, surrounded by a mixture of lamellar α phase and β phase. The nodular α particles have a mean equivalent diameter of 7-8 µm for the as-extruded state and 11-14 µm for the as-forged state. The amount of β phase is lightly lower for the as-extruded state; i.e. 6.5 % against 9 % for the as-forged state.

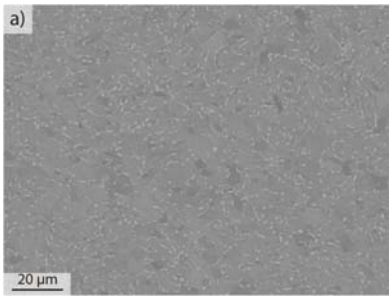

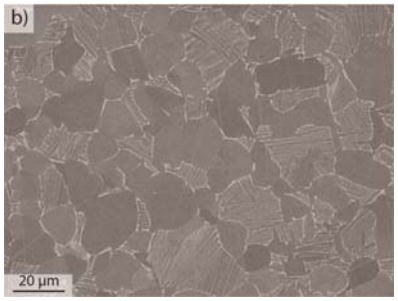

Figure 2. As-received microstructures of TA6V titanium alloy: a) as-extruded state; b) as-forged state.

3.2 Transformation on heating

The variations of α phase amount versus temperature are shown in Figure 3 for both states. The heating conditions were: 10°C/s up to 925°C. The phase amount was determined by HEXRD. The α mass fraction at the initial state is 94.5 % for the extruded state and 92 % for the forged state and is in agreement with the values obtained by image analysis. For the extruded state, the mass fraction remains constant up to 650°C. Despite of the high heating rate, a rapid decrease in α amount is obtained from 94.5% to 50%, namely from 750°C to 925°C. The forged state has a similar behaviour. The dissolution begins at temperatures slightly lower than 600°C and the kinetics is accelerated at 700°C. Moreover a change in the slope is observed at 850°C.

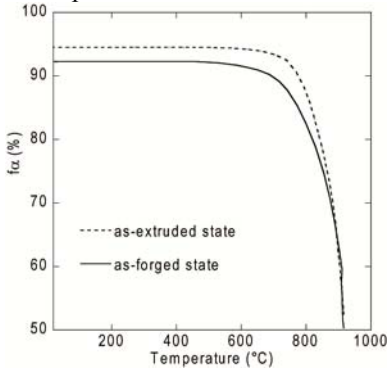

Figure 3. Comparison of α phase amount measured by XRD on heating for the both alloys.

The electrical resistivity variations versus temperature are reported in Figure 4 and are compared to mass fraction of α phase measured by HEXRD in the temperature range 600°C-925°C.

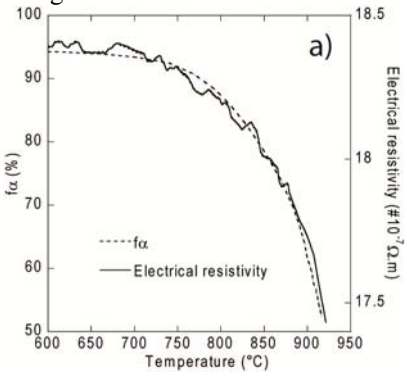

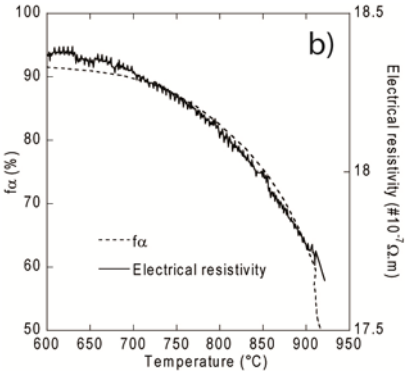

Figure 4. Variations of mass fraction of α phase and electrical resistivity versus temperature. a) extruded state; b) forged state.

In both cases, the dissolution of α phase corresponds to a strong decrease of the electrical resistivity, that amplitude is nearly the same. These good correlations confirm once more the validity of resistivity measurements in analyzing the transformations kinetics.

3.3 Transformation during isothermal holding

The evolutions of mass fraction of α phase during isothermal holding at 925°C are reported in Figure 5. The dissolution kinetics of α phase is similar for both states. Indeed, a rapid evolution is observed at first, followed by a slower regime. The equilibrium state seems reached after about 40 min for the forged state while the amount of α phase decreases continuously with the holding time for the extruded state. It must be emphasized that the amount of dissolved α phase during isothermal holding is low in comparison with the amount dissolved during heating. It represents 20% of the total dissolution.

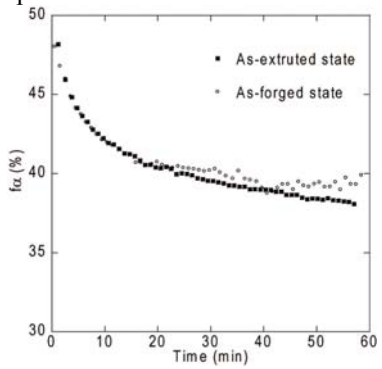

Figure 5. Comparison of α phase amount measured by HEXRD during isothermal holding at 925°C (T_β-70°C).

As for the dissolution kinetics on heating, we have compared the HEXRD results and the changes in electrical resistivity. The isothermal variations in α phase have been normalised and compared to the normalised electrical resistivity variations for the extruded state (Figure 6). A good correlation is again observed between the kinetics obtained by both methods.

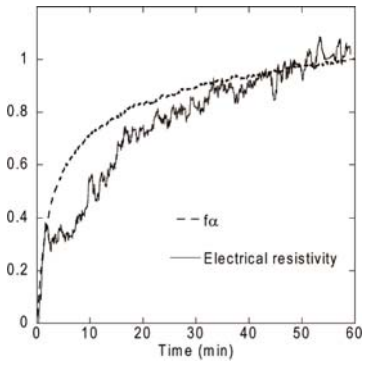

Figure 6. Normalised variations of mass fraction of α phase and electrical resistivity during isothermal holding at 925°C for extruded state.

3.4. Quantitative characterisation after quenching

The microstructure after each isothermal holding for the forged state has been quantified by image analysis. For the extruded state, only specimen hold at T_β-40°C has been quantitatively characterized. Table 1 summarises the isothermal conditions and gives several microstructural features i.e. fraction of nodular α phase (FN_α) and fraction of lamellar α phase (FL_α), number density (NN_α), mean equivalent diameter (m.e.d.) and shape factor (SF) of nodular α phase.

As expected the α phase amount (nodular and lamellar), the number density and the mean equivalent diameter decrease when increasing the holding temperature. The shape factor remains relatively constant. We also observe that fraction of lamellar α decreases more rapidly in comparison with that of nodular morphology. In fact, all the lamellar α phase (41%) is dissolved between T_β-125°C and T_β-40°C while only 29 % of nodular α phase is dissolved in the same temperature range. This finding agrees with the kinetics change revealed by HEXRD and electrical resistivity where the kinetics is accelerated from 700°C with a change of slope at 850°C.

The α amount measured at room temperature by image analysis for specimen hold 1 hour at T_β- 70°C (46%) is close to that measured in real time by XRD after 1 hour at T_β- 70°C (37%). In addition, it can be noticed that the amount of nodular α phase are equivalent for T_β-25°C and T_β-40°C while their number density and their m.e.d differ. This result suggests a growth of nodular α phase during quenching in spite of a high cooling rate (i.e. 50°C/s between 925°C and 800°C).

Table 1. Quantitative data obtained by image analysis after isothermal holding for forged state.

State	FN_α (%)	FL_α (%)	NN_α (#.10^{-3}/μm²)	m.e.d. (μm)	SF
As-forged	50	41	5.5	10.8	0.70
T_β-125°C	47	22	7.7	8.8	0.68
T_β-70°C	37	9	7	8.2	0.66
T_β-40°C	21	0	5.1	7.2	0.65
T_β-25°C	20	0	4.6	7.4	0.65

Table 2 reports the microstructural features after isothermal holding at T_β-40°C for the extruded state. The amount of α phase is close to 20 %, value comparable at the one obtained for the forged state (same holding conditions). As for the initial state, the extruded state exhibits a higher number density and a lower mean equivalent diameter. These results evidence that the differences in the initial microstructure are maintained.

Table 2. Quantitative data obtained by image analysis after isothermal holding for as-forged state.

State	FN_α (%)	FL_α (%)	NN_α (#.10^{-3}/μm^2)	m.e.d. (μm)	SF
T_β-40°C	18.2	0	13.1	4.2	0.65

4. Discussion

The dissolution of α phase during heating and isothermal holding has been investigated by coupling HEXRD, electrical resistivity variations and image analysis. HEXRD results, confirmed by electrical resistivity measurements show that the dissolution kinetics is very rapid on heating in spite of a high heating rate. The complementary approach by HEXRD and image analysis shows that the dissolution kinetics of α lamellar morphology is more rapid as compared with the α nodular one.

Based on present observations, the dissolution kinetics of α phase measured by HEXRD has been compared with equilibrium values calculated by using ThermoCalc software and Saunders titanium public database[7] (Figure 7). As expected, the thermodynamic equilibrium is not reached after heating but the values obtained experimentally are quite close from predicted by ThermoCalc. This comparison consolidates the fact that the dissolution kinetics of α phase is very rapid on heating.

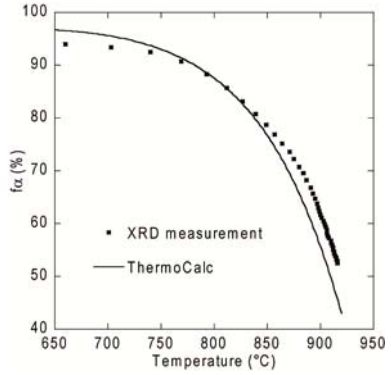

Figure 7. Mass fraction of α phase vs temperature for as-extruded alloy. Calculated line compare to experimental data given as symbols.

In the case of initial as-forged state which contains two different morphologies (lamellar and nodular), the total amounts obtained by HEXRD and predicted by ThermoCalc as a function of temperature are shown in Figure 8. The comparison is quite surprising since the equilibrium amount of α phase predicted by ThermoCalc is above those obtained experimentally up to 850°C. This corresponds principally to the dissolution of lamellar α phase. These results need further studies; however, there is a close connection with the thermo-mechanical process in the α + β domain. In fact, the presence of α phase (nodular) during thermo-mechanical process results to change of the composition in the β region and so the β transus temperature. During cooling, the β region transforms mainly to lamellar α phase with a different chemical composition than that of the nodular α phase formed at high temperature. This means that the difference of composition between the two morphologies will affect strongly the reverse transformation of α to β. This hypothesis has been applied to explain the rapid dissolution of lamellar α phase.

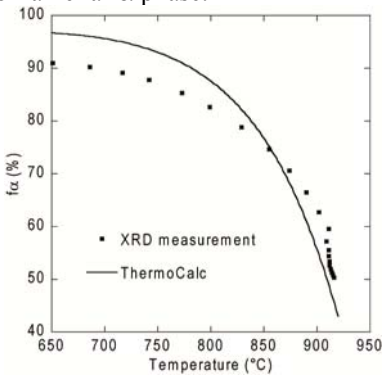

Figure 8. Mass fraction of α phase vs temperature for as-forged alloy. Calculated line compare to experimental data given as symbols.

5. Conclusion

The kinetics of α phase dissolution during heating and isothermal holding has been studied in TA6V alloy which presents initially two different microstructural states. Both lamellar and nodular morphologies dissolve very quickly on heating in spite of a high heating rate with a higher kinetics for lamellar morphology. The comparison of these results with the calculation shows that to predict kinetics of α phase dissolution, it is necessary to take into account the thermo-mechanical history.

Acknowledgements

The authors gratefully acknowledge financial support from AIRBUS and TIMET UK for providing the alloys.

REFERENCES

1) G. Lütjering, Materials Science and Engineering A. 1998; **243**: pp. 32-45.
2) P. Di Napoli, B. Appolaire, E. Aeby-Gautier and A. Bénéteau, Solid State Phenomena. In press.
3) P.C. Collins, B. Welk, T. Searles, J. Tiley, J.C. Russ and H.L. Fraser, Materials Science and Engineering A. 2009; **508**: pp. 174-182.
4) F. Bruneseaux, E. Aeby-Gautier, G. Geandier, J. Teixeira, B. Appolaire, P. Weisbecker and A. Mauro, Materials Science and Engineering A. 2008; **476**: pp. 60-68.
5) S. Malinov, P. Markovsky, W. Sha and Z. Guo, Journal of Alloys and Compounds. 2001; **314**: pp. 181-192.
6) J.D. Miller and S.L. Semiatin, Metallurgical and Materials Transactions A. 2005; **36A**: pp. 259-262.
7) Saunders N., Database for titanium systems, Thermotech Ltd., U.K.